



Original article

Synthesis, crystal structure and pharmacological evaluation of two new Cu(II) complexes of 2-oxo-1,2-dihydroquinoline-3-carbaldehyde (benzoyl) hydrazone: A comparative investigation

Duraisamy Senthil Raja^a, Nattamai S.P. Bhuvanesh^b, Karuppannan Natarajan^{a,*}

^a Department of Chemistry, Bharathiar University, Coimbatore 641046, Tamil Nadu, India

^b Department of Chemistry, Texas A&M University, College Station, TX 77842, USA

ARTICLE INFO

Article history:

Received 20 July 2011

Received in revised form

11 October 2011

Accepted 11 October 2011

Available online 20 October 2011

Keywords:

Copper(II) complexes

DNA binding

Protein binding

Antioxidant

Cytotoxicity

ABSTRACT

Two new copper(II) complexes have been synthesized by reacting 2-oxo-1,2-dihydroquinoline-3-carbaldehyde (benzoyl) hydrazone (H₂L) with CuCl₂·2H₂O or Cu(NO₃)₂·3H₂O. The structures of the complexes have been determined by single crystal X-ray diffraction studies. Results obtained using spectroscopic methods strongly suggested that the ligand and its Cu(II) complexes could interact with calf thymus DNA through intercalation. In the case of protein binding, the obtained results indicated that all the three compounds could quench the intrinsic fluorescence of bovine serum albumin through static quenching process. In addition, antioxidant activity tests showed that H₂L and its copper(II) complexes possess significant scavenging effect against free radicals. Further, the two copper(II) complexes exhibited effective cytotoxic activity against a panel of human cancer cell lines.

© 2011 Elsevier Masson SAS. All rights reserved.

1. Introduction

In the last few decades a renewed interest in metal-based therapy has been raised: in fact, on coordination, not only bioactive ligands might improve their bioactivity profiles, but also inactive ligands may acquire pharmacological properties [1–6]. In addition, metal-coordination is one of the most efficient strategies in the design of repository, slow-release or long-acting drugs [7]. In this regard, the heterocyclic hydrazones constitute an important class of biologically active ligand molecules which have attracted attention of bio-inorganic and medicinal chemists due to their versatile coordination behaviour and wide range of pharmacological properties [8–11]. In particular, Cu(II) complexes containing heterocyclic hydrazones exhibited wide range of biological and pharmaceutical activities that includes DNA binding and cleavage, antimicrobial, anticancer and antioxidant behavior [12–15]. But, only a less attention has been paid in the study of the structure activity relationship of the copper(II) complexes on their biological activity. In this area, we have recently reported that the copper(II) complexes derived from 2-oxo-

1,2-dihydroquinoline-3-carbaldehyde N-substituted thiosemicarbazones and their structure activity relationship on biological properties such as protein binding, antioxidative and cytotoxic activity [16]. However, the structural and biological properties of hydrazone transition metal complexes derived from 2-oxo-1,2-dihydroquinoline-3-carbaldehyde have not been explored well. This aroused our interest in the synthesis of the ligand, 2-oxo-1,2-dihydroquinoline-3-carbaldehyde (benzoyl) hydrazone, and its copper(II) complexes with a view towards evaluating their structure activity relationship on biological properties such as DNA and protein binding, antioxidative and cytotoxic activity after the recent report of the reaction of 2-oxo-1,2-dihydroquinoline-3-carbaldehyde (benzoyl) hydrazone with Cu(NO₃)₂ [17]. We carried out the same reaction and obtained a different complex for which the structure has been proved by single crystal X-ray studies. Moreover, no work seems to have been done on CuCl₂ with the above ligand. So here in, we report a comparative study of the pharmacological properties of two new Cu(II) complexes synthesized from the same ligand with different Cu(II) salts namely chloride and nitrate. The results were analyzed to find out the suitability of these compounds for understanding the mode of binding with DNA as well as laying a foundation for the rational design of novel, powerful agents for probing and targeting nucleic acids.

* Corresponding author. Tel.: +91 422 2428319; fax: +91 422 2422387.

E-mail address: k_nataraj6@yahoo.com (K. Natarajan).

2. Results and discussion

2.1. Synthesis and characterization

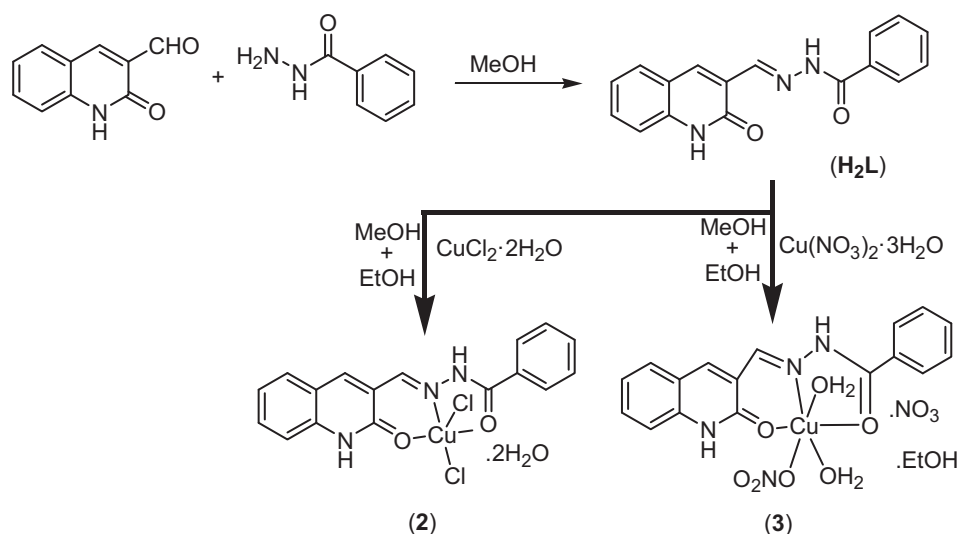
The synthetic routes of the ligand (**1**), 2-oxo-1,2-dihydroquinoline-3-carbaldehyde (benzoyl) hydrazone (H_2L) and its corresponding copper(II) complexes have been sketched out in Scheme 1. The ligand (H_2L) was synthesized from the condensation reaction between 2-oxo-1,2-dihydroquinoline-3-carbaldehyde and benzohydrazide in methanol medium. Corresponding copper(II) hydrazone complexes were obtained by the direct reaction of the ligand with copper(II) salts, $CuCl_2 \cdot 2H_2O$ or $Cu(NO_3)_2 \cdot 3H_2O$ in the mixture of methanol and ethanol under reflux conditions. The single crystals of new copper(II) complexes were isolated by slow evaporation of the reaction mixture over a period of 30–32 days. All the compounds are air stable for extended periods and remarkably soluble in methanol, ethanol, DMF and DMSO. Unlike **1** and **2**, **3** is highly soluble in water. The synthesized compounds were then characterized by elemental analysis, IR, and 1H NMR spectroscopic techniques. The IR peak shift of $\nu_{C=O}$ and $\nu_{C=N}$ vibrations of the ligand gave an idea about the involvement of the ligand in the coordination with copper ion. The experimental values of μ_{eff} i.e., 1.77 and 1.74 for $[CuCl_2(H_2L)] \cdot 2H_2O$ (**2**) and $[Cu(NO_3)(H_2L)(H_2O)_2]NO_3 \cdot C_2H_5OH$ (**3**) respectively revealed the presence of +2 oxidation state of copper. The solid state structures of the new copper(II) complexes were determined by single crystal X-ray crystallographic studies.

2.2. X-ray structural characterization

The perspective ORTEP view of $[CuCl_2(H_2L)] \cdot 2H_2O$ with atom numbering scheme is shown in Fig. 1. Details of the data collection and the parameters of refinement process are presented in Table 1. Selected bond lengths and angles are summarized in Table 2. The ligand is coordinated to the copper ion in a neutral manner via ONO donor atoms and the rest of the two coordination sites are occupied by chloride ions completing a square pyramidal geometry around the central metal ion in complex **2**. Analysis of the shape determining angles, α and β (the two largest angles around the central atom) [18] yields a value for the trigonality index, τ [$\tau = (\alpha - \beta)/60$], of 0.0525. According to it ($\tau = 0$ and 1 for perfect square pyramidal and trigonal bipyramidal geometries, respectively), the geometry

around Cu(II) can be described as a slightly distorted square pyramid. The copper(II) ion lies at about 0.185 Å above the average basal plane towards the axial Cl2 atom. The dihedral angle between the mean planes of the five-membered chelate ring and the six-membered one is 5.09°. In addition, there is an appreciable Jahn–Teller effect highlighted by an axial Cu–Cl2 distance (2.688(2) Å) significantly longer than that observed for equatorial Cu–Cl1 distance (2.2274(17) Å). Since the hydrazone moieties possess both the hydrogen bond donors as well as acceptors, the species provide the possibility of forming hydrogen bonds in the crystal. In fact, the crystal lattice of the complex showed a two dimensional array in which each unit of the complex is hydrogen bonded to the other involving N2 and N3 nitrogen atoms, O30 and O40 oxygen atoms and the Cl1 and Cl2 chlorine atoms.

Molecular structure of the cationic complex $[Cu(NO_3)(H_2L)(H_2O)_2]NO_3$ (H_2L)(H_2O) $_2$]NO $_3$ together with the atom-labeling scheme is depicted in Fig. 2. The crystallographic data with selected bond lengths and bond angles are listed in Tables 1 and 2. The crystal structure of **3** consists of discrete $[Cu(NO_3)(H_2L)(H_2O)_2]^+$ cations and nitrate anions with six donor atoms in an octahedral fashion (4 + 2) surround the copper(II) ion in the complex. The basal plane is made up from the O, N, and O atoms of the neutral tridentate ligand and one oxygen atom of the water molecule, while the oxygen from another water molecule has taken one of the apical vertices, the remaining apical vertex has been occupied by one of the oxygens of the nitrate ion. Here, Cu(II) ion lies at 0.090 Å above the average basal plane towards the apical oxygen of water molecule. The dihedral angle between the mean planes of the five-membered chelate ring and the six membered one is 3.46° which ensures that the planarity of square should be appreciable. The axial Cu–O25 bond length (2.324(3) Å) is longer than that of basal Cu–O20 bond length (1.935(3) Å) which can be ascribed to Jahn–Teller distortion in **3**. The molecular packing suggests that the stabilization of the lattice must have been due to several hydrogen bonds, mainly involving the N2, N3, O20, O25, O31, O32, O42, O43 and O50 atoms. It is to be noted that in the X-ray structural analysis, though two water molecules are present in **2**, the occupancy factor for one of them was found to be 0.50; but in the case of **3** the occupancy factor for the ethanol is 0.70. Important bond lengths and angles for both the complexes are summarized in the Table 2 which agree well with those found in Cu(II) complexes reported earlier [15–17].



Scheme 1. The synthetic routes of the ligand and its Cu(II) complexes.

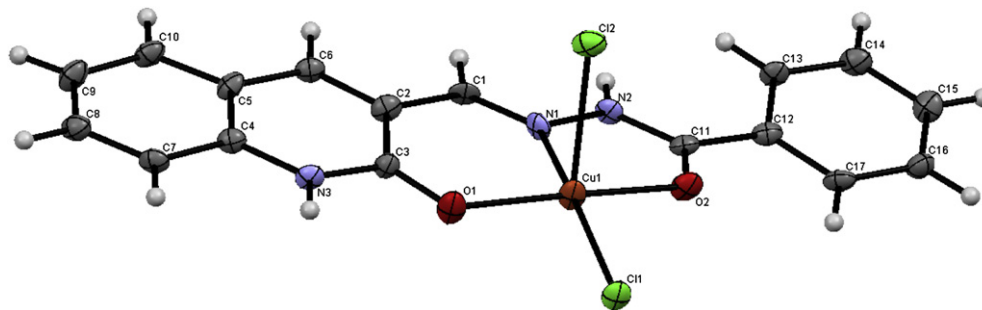


Fig. 1. ORTEP view of the molecular structure and atom-labeling scheme of **2**. Thermal ellipsoids are drawn at 50% probability level. Water molecules have been omitted for clarity.

2.3. DNA interaction studies

It is a well-known fact that DNA is an important genetic substance in organism and its regions involved important processes, such as gene expression, gene transcription, mutagenesis and carcinogenesis [19]. Moreover, DNA is an important cellular receptor, many compounds exert their antitumor effects through binding to DNA thereby changing the replication of DNA and inhibiting the growth of the tumor cells, which is the basis of designing new and more efficient antitumor drugs and their effectiveness depends on the mode and affinity of the binding [20–23]. Therefore, binding studies of small molecules to DNA are considered to be more important in the development of DNA molecular probes and new therapeutic reagents [24,25].

2.3.1. Electronic absorption titration

Electronic absorption spectroscopy is one of the most commonly used techniques for the investigation of the binding

mode of small molecules to DNA [26]. Intercalative mode of binding usually results in hypochromism along with or without small red or blue shift due to the strong stacking interaction between an aromatic chromophore and the base pairs of DNA. The extent of shift and hypochromism are commonly found to correlate with the intercalative binding strength. But, metal complexes which bind non-intercalatively or electrostatically with DNA may result in hyperchromism or hypochromism [26–28]. The absorption spectra of the ligand (**1**) and its complexes **2** and **3** in the absence and presence of calf thymus DNA (CT-DNA) (at a constant concentration of compounds) are shown in Fig. 3. Absorption spectra of the metal hydrazone complexes exhibited intra ligand charge transfer (ILCT), ligand - to - metal charge transfer (LMCT), and metal - to - ligand charge transfer (MLCT) transitions. Upon incremental additions of DNA to the test compounds, the followings changes were observed. In the presence of DNA, the absorption bands of the ligand (**1**) exhibited hypochromism of about 5.99% and 5.52% respectively at 326 and 363 nm. However, Complex **2** exhibited the hypochromism

Table 1

Experimental data for crystallographic analyses.

	2	3
Empirical formula	C ₁₇ H ₁₆ Cl ₂ Cu N ₃ O _{3.50}	C _{18.40} H _{21.20} Cu N ₅ O _{10.70}
Formula weight	452.77	547.14
Temperature (K)	110(2)	110(2)
Wavelength (Å)	0.71073	0.71073
Crystal system	Monoclinic	Monoclinic
Space group	P2(1)/n	P2(1)/c
Unit cell dimensions		
a (Å)	7.672(5)	13.122(6)
b (Å)	9.762(6)	11.311(5)
c (Å)	23.585(15)	15.519(7)
α (°)	90	90
β (°)	92.450(9)	103.688(6)
γ (°)	90	90
Volume (Å ³)	1765(2)	2238.1(18)
Z	4	4
Density (calc.) (Mg/m ³)	1.704	1.624
Abs. coefficient (mm ⁻¹)	1.567	1.046
F(000)	920	1125
Crystal size (mm ³)	0.46 × 0.45 × 0.16	0.50 × 0.46 × 0.31
Index ranges	-9 ≤ h ≤ 9, -12 ≤ k ≤ 12, -30 ≤ l ≤ 30	-16 ≤ h ≤ 16, -14 ≤ k ≤ 14, -20 ≤ l ≤ 20
Reflections collected	17981	24721
Independent reflections	3991 [R(int) = 0.0965]	5068 [R(int) = 0.0343]
Absorption correction	Semi-empirical from equivalents	Semi-empirical from equivalents
Max. and min. transmission	0.7876 and 0.5326	0.7376 and 0.6229
Refinement method	Full-matrix least-squares on F ²	Full-matrix least-squares on F ²
Data/restraints/parameters	3991/0/244	5068/0/325
Goodness-of-fit on F ²	1.016	1.041
Final R indices [I > 2σ(I)]	R1 = 0.0684, wR2 = 0.1661	R1 = 0.0538, wR2 = 0.1427
R indices (all data)	R1 = 0.0831, wR2 = 0.1731	R1 = 0.0611, wR2 = 0.1488
CCDC number	784286	830873

Table 2
Selected bond lengths (Å) and angles (°) for the complexes **2** and **3**.

	2	3
Cu(1)–O(1)	1.938(4)	1.927(2)
Cu(1)–O(2)	1.963(4)	1.971(2)
Cu(1)–N(1)	1.990(4)	1.951(3)
Cu(1)–Cl(1)	2.2274(17)	
Cu(1)–Cl(2)	2.688(2)	
Cu(1)–O(20)		1.935(3)
Cu(1)–O(25)		2.324(3)
Cu(1)–O(33)		2.631
O(1)–Cu(1)–O(2)	169.54(16)	173.80(10)
O(1)–Cu(1)–N(1)	91.72(16)	92.60(11)
O(2)–Cu(1)–N(1)	80.71(16)	81.52(9)
O(1)–Cu(1)–Cl(1)	92.13(12)	
O(2)–Cu(1)–Cl(1)	93.66(12)	
N(1)–Cu(1)–Cl(1)	166.39(13)	
O(1)–Cu(1)–Cl(2)	92.83(13)	
O(2)–Cu(1)–Cl(2)	93.85(12)	
N(1)–Cu(1)–Cl(2)	86.33(13)	
Cl(1)–Cu(1)–Cl(2)	106.51(5)	
O(1)–Cu(1)–O(20)		92.36(12)
O(20)–Cu(1)–O(2)		93.18(11)
O(20)–Cu(1)–N(1)		170.25(11)
O(1)–Cu(1)–O(25)		88.29(11)
O(20)–Cu(1)–O(25)		95.23(11)
N(1)–Cu(1)–O(25)		93.31(11)
O(2)–Cu(1)–O(25)		93.97(10)

of about 41.04%, 56.44%, 55.09% and 52.76% with hypsochromic shift of 2, 1, 2 and 1 nm at 261, 365, 401 and 423 nm respectively. On the other hand, the absorption bands of **3** at 260, 366, 400 and 421 nm exhibited the same phenomenon of hypsochromism of about 58.22%, 68.42%, 69.35% and 68.41% with hypsochromic shift of about 3, 1, 2 and 1 nm respectively. These results suggested an intimate association of the test compounds with CT-DNA and it is also likely that these compounds bind to the DNA helix via intercalation [29]. After the compounds intercalate to the base pairs of DNA, the π^* orbital of the intercalated compounds could couple with π orbitals of the base pairs, thus decreasing the $\pi \rightarrow \pi^*$ transition energies. Therefore, these interactions resulted in the observed hypsochromism [30]. The complexes **2** and **3** showed more

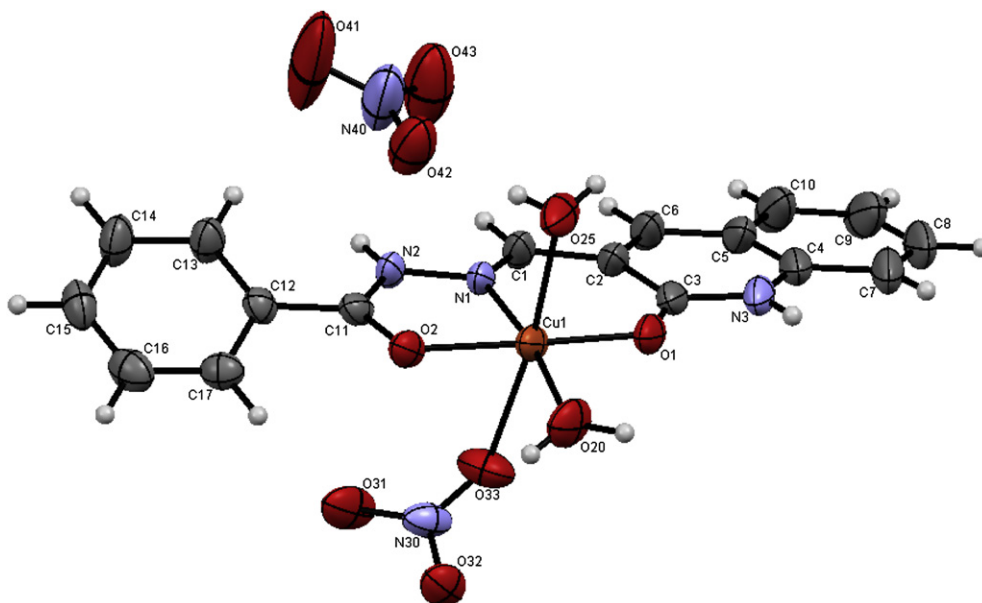
hypochromicity than the ligand, indicating that the binding strength of the copper(II) complexes are much stronger than that of the free ligand. In order to compare quantitatively the binding strength of the compounds, the intrinsic binding constants (K_b) of them with CT-DNA were determined from the following equation [31],

$$[\text{DNA}]/(\epsilon_a - \epsilon_f) = [\text{DNA}]/(\epsilon_b - \epsilon_f) + 1/K_b(\epsilon_b - \epsilon_f)$$

where [DNA] is the concentration of DNA in base pairs, the apparent absorption coefficient ϵ_a , ϵ_f and ϵ_b correspond to $A_{\text{obs}}/[\text{compound}]$, the extinction coefficient of the free compound and the extinction coefficient of the compound when fully bound to DNA, respectively. The plot of $[\text{DNA}]/(\epsilon_a - \epsilon_f)$ versus [DNA] gave a slope and the intercept which are equal to $1/(\epsilon_b - \epsilon_f)$ and $1/K_b(\epsilon_b - \epsilon_f)$, respectively; K_b is the ratio of the slope to the intercept. The magnitudes of intrinsic binding constants (K_b) were calculated to be $6.367 \times 10^4 \text{ M}^{-1}$, $2.137 \times 10^5 \text{ M}^{-1}$ and $6.724 \times 10^5 \text{ M}^{-1}$ for the compounds **1**, **2**, and **3** respectively. The observed values of K_b revealed that the ligand and the Cu(II) complexes bind to DNA via intercalative mode [29,30]. From the results obtained, it has been found that the complex **3** strongly bound with CT-DNA than that of **2** and **1** and the order of binding affinity is $1 < 2 < 3$. From the electronic absorption studies, though it has been found that the three compounds can bind to DNA by intercalation, the binding mode need to be proved through some more experiments.

2.3.2. Fluorescence titration

To further confirm the interactions between the test compounds and CT-DNA, emission experiments were carried out. The results of fluorescence titration spectra have been confirmed to be effective for characterizing the binding mode of the metal complexes to DNA [32,33]. The results of the emission titration for the ligand and its corresponding complexes with CT-DNA that are illustrated in the titration curves are shown in Fig. 4. Increase in DNA concentration increases the emission intensity of the compounds **1**, **2** and **3**. Upon incremental additions of CT-DNA, the emission intensity of the ligand at 437 nm increased around 1.18 times on comparison of the same in the absence of DNA whereas for its corresponding



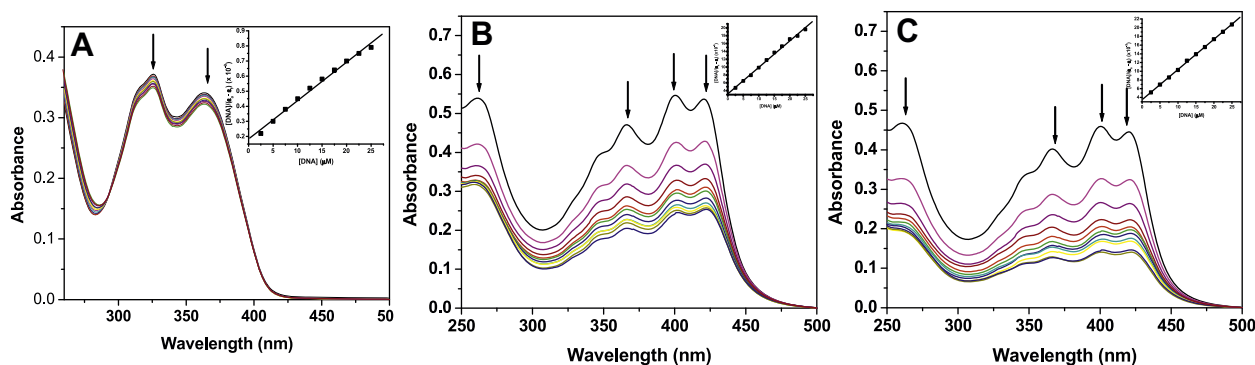


Fig. 3. Absorption spectra of compounds **1** (A), **2** (B) and **3** (C) (25 μM) in the presence of increasing amounts of CT-DNA (0, 2.5, 5, 7.5, 10, 12.5, 15, 17.5, 20, 22.5, 25 μM ; subsequent spectra). Arrows show the absorbance changes upon increasing DNA concentration. Inset: Plots of $[\text{DNA}]/(\epsilon_a - \epsilon_f)$ versus $[\text{DNA}]$ for the compounds with CT-DNA.

complexes **2** and **3** at 452 and 450 nm the intensities were increased by around 1.31 and 2.06 times respectively. This phenomenon is related to the extent to which the compound penetrates into the hydrophobic environment inside the DNA, thereby avoiding the quenching effect of solvent water molecules. The binding of free ligand and complexes **2**, **3** to CT-DNA leads to a marked increase in the emission intensity, which also agrees with those observed for other intercalators [15,17]. These results show that the complexes bound more strongly than the free ligand. From the observed intensity enhancement of the two complexes in the presence of CT-DNA, it can be seen that **3** has more DNA-binding ability than **2**. The higher binding affinity of the Cu(II) complexes is attributed to the extension of the π system of the intercalated ligand due to the coordination to Cu(II) ion. Since the complexes have greater planar area than that of the free ligand, the complexes penetrate more deeply into, and stacking more strongly with the base pairs of the DNA.

2.3.3. Competitive binding between ethidium bromide and the compounds for CT-DNA

Steady-state competitive binding experiments using the compounds **1**, **2** and **3** as quenchers were undertaken to get further proof for the binding of the compounds to DNA via intercalation. Ethidium bromide (EB) is a planar cationic dye which is widely used as a sensitive fluorescence probe for native DNA. EB emits intense fluorescent light in the presence of DNA due to its strong intercalation between the adjacent DNA base pairs [34,35]. The displacement technique is based on the decrease of fluorescence resulting from the displacement of EB from a DNA sequence by a quencher and the quenching is due to the reduction of the number of binding sites on the DNA that is available to the EB. The fluorescence quenching spectra of DNA-bound EB by compounds **1**, **2** and **3**

shown in Fig. 5 illustrate that as the concentration of the compounds increases, the emission band at 602 nm exhibited hypochromism up to 14.75, 23.00 and 47.04% of the initial fluorescence intensity for **1**, **2** and **3** respectively. The observed decrease in the fluorescence intensity clearly indicates that the EB molecules are displaced from their DNA binding sites and are replaced by the compounds under investigation [36]. Quenching data were analyzed according to the following Stern–Volmer equation,

$$I_0/I = K_q[Q] + 1$$

where I_0 is the emission intensity in the absence of quencher, I is the emission intensity in the presence of quencher, K_q is the quenching constant, and $[Q]$ is the quencher concentration. The K_q value is obtained as a slope from the plot of I_0/I versus $[Q]$.

The quenching plots illustrate that the quenching of EB bound to CT-DNA by free ligand (**1**), complexes **2** and **3** are in good agreement with the linear Stern–Volmer equation. In the Stern–Volmer plots (Fig. 5D) of I_0/I versus $[Q]$, the quenching constant (K_q) is given by the ratio of the slope to intercept. The K_q values for **1**, **2** and **3** were found to be $1.73 \times 10^3 \text{ M}^{-1}$, $2.70 \times 10^3 \text{ M}^{-1}$ and $8.97 \times 10^3 \text{ M}^{-1}$ respectively. Further, the binding constant (K_{app}) value obtained for the compounds using the following equation,

$$K_{EB}[\text{EB}] = K_{app}[\text{compound}]$$

(where the compound concentration has the value at a 50% reduction of the fluorescence intensity of EB, $K_{EB} = 1.0 \times 10^7 \text{ M}^{-1}$ and $[\text{EB}] = 5 \mu\text{M}$) were $8.65 \times 10^4 \text{ M}^{-1}$, $1.35 \times 10^5 \text{ M}^{-1}$ and $4.48 \times 10^5 \text{ M}^{-1}$ for **1**, **2** and **3** respectively. These data suggested that the interaction of the copper(II) complexes with CT-DNA is stronger than that of the free ligand, which is consistent with the above absorption and emission spectral observations. Since these changes

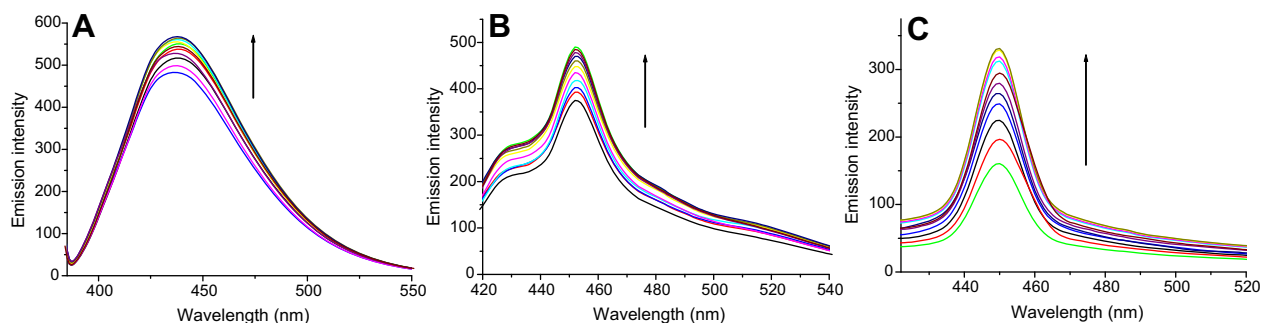


Fig. 4. Emission enhancement spectra of compounds **1** (A), **2** (B) and **3** (C) (25 μM) in the presence of increasing amounts of CT-DNA (0, 2.5, 5, 7.5, 10, 12.5, 15, 17.5, 20, 22.5, 25 μM ; subsequent spectra); Arrow shows the emission intensity increases upon increasing DNA concentration.

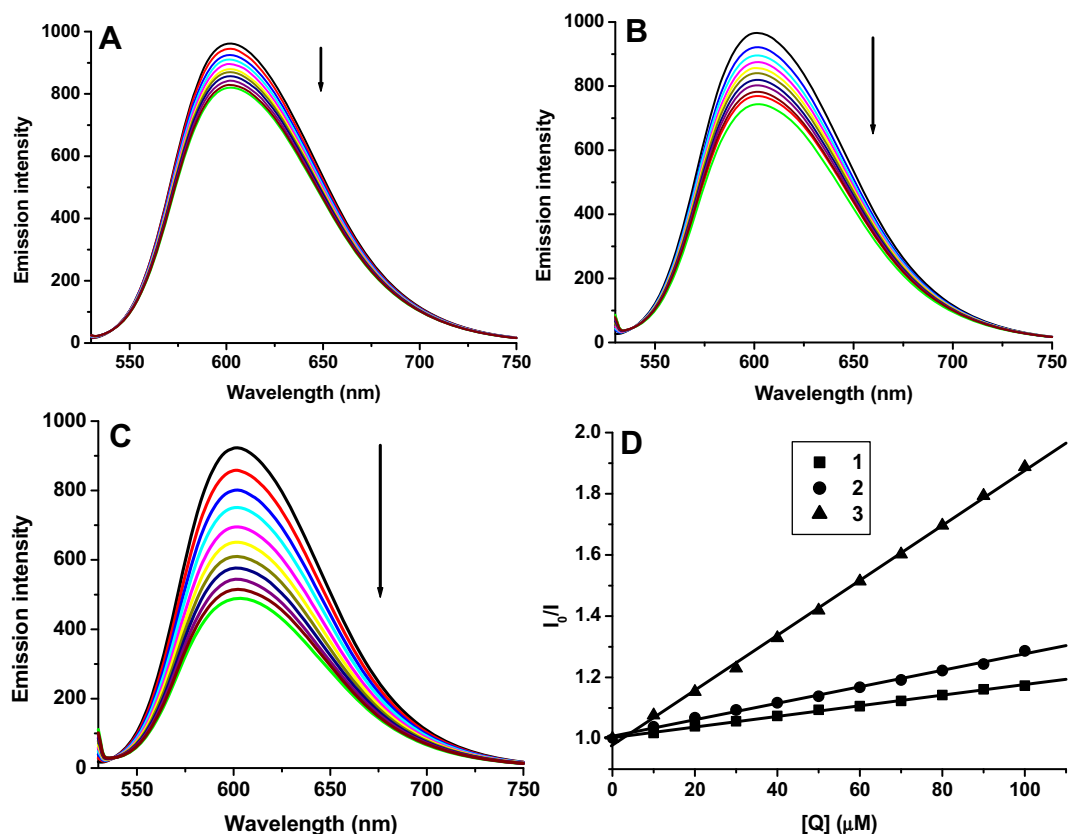


Fig. 5. Emission spectra of DNA-EB system ([DNA] = 10 μ M and [EB] = 5 μ M), λ_{ex} = 510 nm, in the presence of (0, 10, 20, 30, 40, 50, 60, 70, 80, 90, 100 μ M) **1** (A), **2** (B) and **3** (C). Arrow shows the emission intensity changes upon increasing compounds concentration. (D) Stern–Volmer plots of the fluorescence titration of **1**, **2** and **3**.

indicate only one kind of quenching process, it may be concluded that **1**, **2** and **3** bind to CT-DNA via the same mode. Furthermore, such quenching constants and binding constants of the ligand and Cu(II) complexes suggest that the interaction of all the compounds with DNA should be of intercalation [37]. On the basis of all the spectroscopic studies, we concluded that the free ligand and copper(II) complexes can bind to CT-DNA in an intercalative mode and that the Cu(II) complexes bind to CT-DNA more strongly than the free ligand. Though the ligand coordinated as neutral tridentate to Cu(II) in both the complexes containing water and chloride or nitrate as co-ligands, the cationic nature of **3** is likely to be the reason for the observed strong affinity of **3** with DNA over **2**.

2.4. Protein binding studies

2.4.1. Fluorescence quenching of protein by H_2L and its two Cu(II) complexes

Serum albumin is the protein which increases the apparent solubility of drugs in plasma and modulates their delivery to cell. So, it is of important to understand the mechanism of interaction of a bioactive compound with protein. The nature and magnitude of drug–protein interaction influence the biological activity such as efficacy and delivery rate of the drug [38]. In addition, it is also important to study the binding parameters of drugs with protein in order to control the pharmacological response of drugs and design of dosage forms. Serum albumin is considered as a model for studying drug–protein interaction *in vitro* since it is the major binding protein for drugs and other physiological substances. The analysis of chemical compounds bound to bovine serum albumin (BSA) has been carried out by examining the respective fluorescence spectra. Changes in molecular environment in the vicinity of

fluorophore can be accessed by the changes in fluorescence spectra in the absence and presence of the compounds and hence, provide clues for the nature of the binding phenomenon. The interaction of our compounds with BSA protein was studied by fluorescence measurement at room temperature. A solution of BSA (1 μ M) was titrated with various concentrations of the test compounds **1**, **2** and **3** (0–10 μ M). Fluorescence spectra were recorded in the range of 290–440 nm upon excitation at 280 nm. The effect of compounds on the fluorescence emission spectrum of BSA is shown in Fig. 6. Addition of the above compounds to the solution of BSA resulted in significant decrease of the fluorescence intensity of BSA at 344 nm, up to 50.96, 56.90 and 65.81% of the initial fluorescence intensity of BSA accompanied by a hypsochromic shift of 3, 8 and 9 nm for **1**, **2** and **3** respectively. The observed blue shift is mainly due to the fact that the active site in protein is buried in a hydrophobic environment. This result suggested a definite interaction of all the three compounds with the BSA protein.

Quenching can occur by different mechanisms, which are usually classified as dynamic quenching and static quenching; dynamic quenching refers to a process in which the fluorophore and the quencher come into contact during the transient existence of the excited state. Static quenching refers to fluorophore–quencher complex formation in the ground state. A simple method to explore the type of quenching is UV–visible absorption spectroscopy. UV–visible spectra of BSA in the absence and presence of the compounds (Fig. 7) show that the absorption intensity of BSA was enhanced as the compounds were added, and there was a little blue shift of about 1, 2 and 2 nm for **1**, **2** and **3** respectively. It revealed that there exists a static interaction between BSA and the added compounds due to the formation of ground state complex of the type BSA–compound as reported earlier [39]. To study the

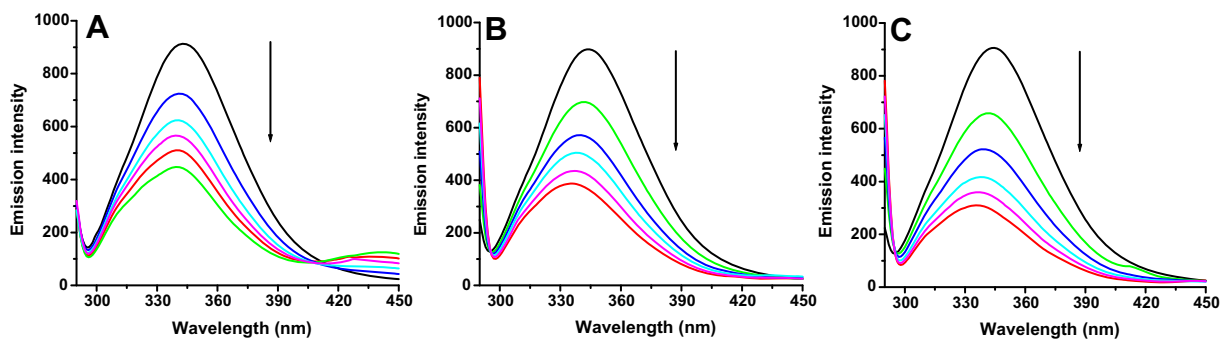


Fig. 6. The emission spectrum of BSA (1 μM ; $\lambda_{\text{exc}} = 280 \text{ nm}$; $\lambda_{\text{emi}} = 344 \text{ nm}$) in the presence of increasing amounts of compounds **1** (A), **2** (B) and **3** (C) (0, 2, 4, 6, 8 and 10 μM). Arrow shows the fluorescence quenching upon increasing concentration of the compounds.

quenching process further, fluorescence quenching data were analyzed with the Stern–Volmer equation and Scatchard equation. The quenching constant (K_q) can be calculated using the plot of I_0/I versus $[Q]$ (Fig. 8A). If it is assumed that the binding of compounds with BSA occurs at equilibrium, the equilibrium binding constant can be analyzed according to the Scatchard equation:

$$\log [(I_0 - I)/I] = \log K_{\text{bin}} + n \log [Q]$$

where K_{bin} is the binding constant of compound with DNA and n is the number of binding sites.

From the plot of $\log [(I_0 - I)/I]$ versus $\log [Q]$ (Fig. 8B), the number of binding sites (n) and binding constant (K_{bin}) have been obtained. The calculated K_q , K_{bin} and n values are given in Table 3. The calculated value of n is around one for all the compounds indicating the existence of a single binding site in BSA for all the compounds. The values of K_q and K_{bin} for **1**, **2** and **3** suggested that the complexes interact with BSA more strongly than the ligand. Among the two Cu(II) complexes, the cationic complex (**3**) has better interaction with BSA than the neutral complex (**2**).

2.4.2. Characteristics of synchronous fluorescence spectra

To investigate the structural changes occurred to BSA upon the addition of our compounds, synchronous fluorescence spectra of BSA were measured before and after the addition of test compounds to get valuable information on the molecular micro-environment, particularly in the vicinity of the fluorophore functional groups [40]. It is a well-known fact that the fluorescence of BSA is normally due to the presence of tyrosine, tryptophan and

phenylalanine residues and hence, spectroscopic methods are usually applied to study the conformation of serum protein. According to Miller [41], in synchronous fluorescence spectroscopy, the difference between excitation and emission wavelength ($\Delta\lambda = \lambda_{\text{emi}} - \lambda_{\text{exc}}$) reflects the spectra of a different nature of chromophores. If the $\Delta\lambda$ value is 15 nm, the synchronous fluorescence of BSA is characteristic of tyrosine residue whereas a larger $\Delta\lambda$ value of 60 nm is characteristic of tryptophan [42]. The synchronous fluorescence spectra of BSA with various concentrations of test compounds were recorded at $\Delta\lambda = 15 \text{ nm}$ and $\Delta\lambda = 60 \text{ nm}$ are shown in Figs. 9 and 10 respectively. In the synchronous fluorescence spectra of BSA at $\Delta\lambda = 15$, addition of the compounds to the solution of BSA resulted in a small decrease of the fluorescence intensity of BSA at 302 nm, up to 22.04% of the initial fluorescence intensity of BSA for **1**; but for the complexes **2** and **3**, an increase in the intensity of the above said band for about 1.43 and 1.25 times respectively. At the same time, in the case of synchronous fluorescence spectra of BSA at $\Delta\lambda = 60$, addition of the compounds to the solution of BSA resulted in significant decrease of the fluorescence intensity of BSA at 342 nm, up to 52.16, 53.30 and 68.41% of the initial fluorescence intensity of BSA for **1**, **2** and **3** respectively. The synchronous fluorescence spectral studies clearly suggested that the fluorescence intensities of both the tryptophan and tyrosine were affected with increasing concentration of the test compounds. The results suggest that the interaction of compounds with BSA affects the conformation of both tryptophan and tyrosine micro-region [8] which indicates the hydrophobicity around tryptophan residues is strengthened. The hydrophobicity observed in fluorescence and synchronous measurements confirmed the effective binding of all the compounds with the BSA.

2.5. Evaluation of antioxidant properties of the compounds

Since the experiments conducted so far revealed that the ligand and its Cu(II) complexes exhibit good DNA and protein binding affinity, it is considered worthwhile to study the radical scavenging properties of these compounds. The antioxidant properties of quinoline derivatives have attracted a lot of interests and have been extensively investigated, mainly in the *in vitro* systems [43,44]. The radical scavenging activities of our compounds along with standards, butylatedhydroxyanisole (BHA) and butylatedhydroxytoluene (BHT) in cell free system have been examined with reference to hydroxyl radicals, 2,2'-diphenyl-1-picrylhydrazyl (DPPH) radicals, nitric oxide, superoxide anion radicals and the determination of 50% activity (IC_{50}) values. It is to be noted that no significant radical scavenging activities were observed in all the experiments carried out with CuCl_2 and $\text{Cu}(\text{NO}_3)_2$, even up to 1.0 mmol of concentration under the same experimental

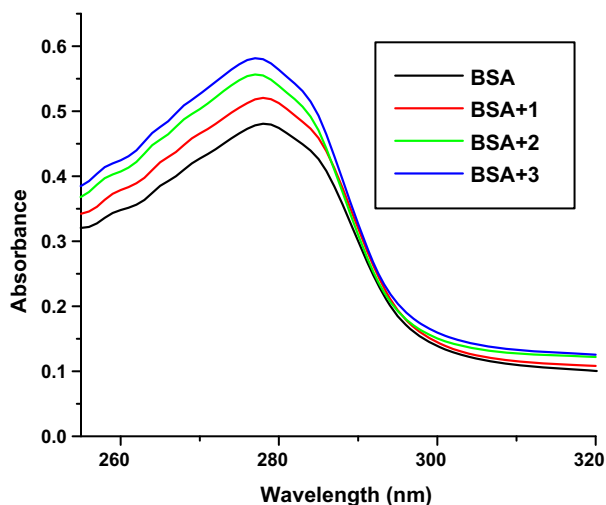


Fig. 7. Absorption spectra of BSA (10 μM), and with compounds, **1**, **2** and **3** (5 μM).

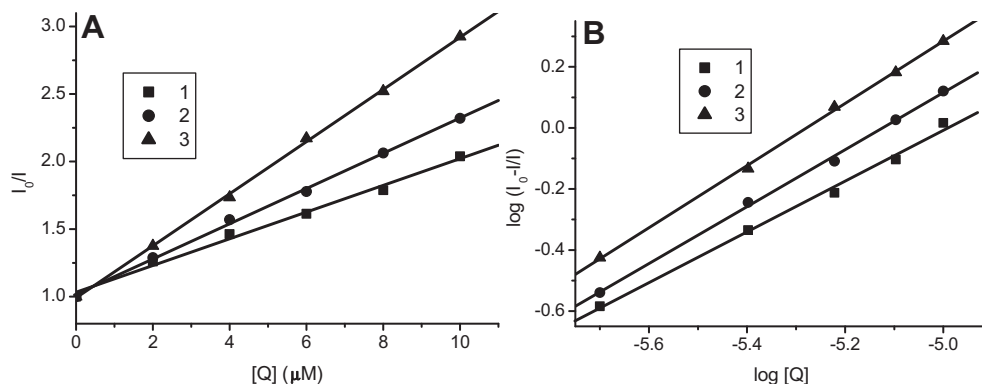


Fig. 8. (A) Stern–Volmer plots of the fluorescence titration of **1**, **2** and **3** with BSA. (B) Scatchard plots of the fluorescence titration of **1**, **2** and **3** with BSA.

conditions. The antioxidant activities of the tested compounds along with the standards at various concentrations have been given in Fig. 11 which showed that a concentration dependent activity was observed. The IC_{50} values (Table 4) indicated that the three compounds showed antioxidant activity in the order of $3 > 2 > 1$ in all the experiments. The DPPH radical scavenging power of the tested compounds was the most and nitric oxide scavenging activity was the least. The scavenging activity results of **2** and **3** are much better than that observed for standard antioxidants BHA and BHT except in the case of DPPH radical scavenging activity which showed almost equal activity for the standards and the two copper(II) complexes. But, the antioxidant activity of **1** was slightly higher than that of the standards in all the cases except in DPPH radical scavenging activity. From the above results, it can be concluded that the scavenging effects of the free ligand is significantly less when compared to that of their corresponding Cu(II) complexes which is due to the chelation of the organic ligand with the Cu(II) ion. Moreover, from the results obtained for the two Cu(II) complexes, it can be inferred that the difference in the nature of the complex is likely to induce variations in antioxidant activities. Among the two Cu(II) complexes, the highest activity for **3** might be due to the cationic nature of the octahedral complex (**3**) over the neutral square pyramidal complex (**2**).

2.6. Cytotoxic activity evaluation of the compounds

The positive results obtained from the previous biological studies namely, DNA binding, BSA binding and antioxidative studies of compounds **1**, **2** and **3** encouraged us to test their cytotoxicity against a panel of human cancer cell lines (human cervical cancer cell line (HeLa), human laryngeal epithelial carcinoma cells (HEp-2), and human liver carcinoma cells (Hep G2)) along with one normal mouse embryonic fibroblasts cell line (NIH 3T3). Compounds **1**, **2** and **3** were dissolved in DMSO and blank samples containing same volume of DMSO are taken as controls to identify the activity of solvent in this cytotoxicity experiment. Cisplatin was used as a positive control to assess the cytotoxicity of the test compounds. The results were analyzed by means of cell viability

expressed as IC_{50} values are shown in Table 5. The ligand did not show any significant activity even up to 400 μ M of concentration on all the cells. However, complexes **2** and **3** showed excellent activity on the three cancer cells. The IC_{50} values for **3** demonstrated a much higher inhibitory effect than **2**. The results of *in vitro* cytotoxic activity studies indicate that the two Cu(II) complexes have excellent activities against human cancer cells than the corresponding ligand but showed significantly less activity than cisplatin. In addition, IC_{50} values of all the compounds against NIH 3T3 mouse embryonic fibroblasts (normal cells) are found to be above 200 μ M which confirmed that the compounds are very specific on cancer cells. But, copper(II) chloride and copper(II) nitrate did not show any significant activity even up to 300 μ M of concentration on all the cells which confirmed that the chelation of the ligand with the Cu(II) ion is the only responsible factor for the observed cytotoxic properties of the new complexes [45–47]. The two Cu(II) complexes which possess better cytotoxic activities than ligand may be attributed to the extended planar structure induced by the $\pi \rightarrow \pi^*$ conjugation resulting from the chelating of the metal ion with ligand. In addition, though the ligand coordinated as neutral tridentate to Cu(II) in both the complexes, the inhibitory activity of **3** against cancer cells is higher than **2**, which may be due to the cationic nature of the complex.

3. Conclusion

Two new copper(II) complexes have been synthesized by reacting 2-oxo-1,2-dihydroquinoline-3-carbaldehyde (benzoyl) hydrazone with $CuCl_2 \cdot 2H_2O$ or $Cu(NO_3)_2 \cdot 3H_2O$. Single crystal X-ray diffraction studies revealed that the structure of the new copper(II) chloride complex, $[CuCl_2(H_2L)] \cdot 2H_2O$ (**2**) is a square pyramid and copper(II) nitrate complex, $[Cu(NO_3)(H_2L)(H_2O)_2]NO_3 \cdot C_2H_5OH$ (**3**) is octahedral. Though the change of counter ion (Cl^- to NO_3^-) in Cu(II) salts did not alter the coordination mode of hydrazone ligand, there was a change in the geometry from square pyramidal to an octahedral one along with a change from neutral to cationic form of the resulting Cu(II) complexes. The DNA-binding properties of the free ligand and two Cu(II) complexes were investigated by absorption and fluorescence measurements. The results supported the fact that the compounds bind to CT-DNA via intercalation. The binding constants show that the DNA binding affinity increased in the order $1 < 2 < 3$. The protein binding properties of the compounds examined by the fluorescence spectra suggested that the binding affinity of cationic complex (**3**) to BSA is stronger than that of neutral complex (**2**) and the ligand. In addition, the compounds also exhibited good antioxidant activities and the activity of **3** is better than that of **2** and **1**. Moreover, the complexes **2** and **3** showed considerable cytotoxic activity against HeLa, HEp-2 and Hep G2

Table 3

Quenching constant (K_q), binding constant (K_{bin}) and number of binding sites (n) for the interactions of compounds with BSA.

Compound	K_q (M^{-1})	K_{bin} (M^{-1})	n
1	9.896×10^4	1.409×10^4	0.831
2	1.304×10^5	6.036×10^4	0.933
3	1.929×10^5	2.380×10^5	1.019

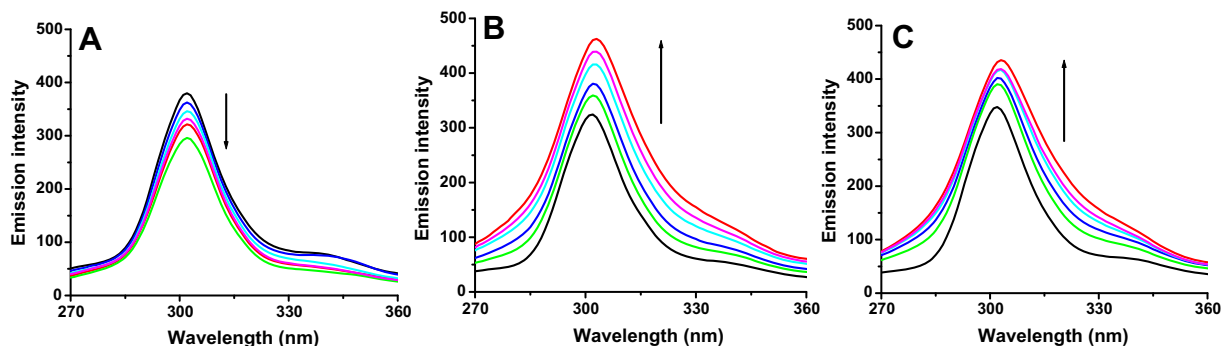


Fig. 9. Synchronous spectra of BSA (1 μM) in the presence of increasing amounts of compounds **1** (A), **2** (B) and **3** (C) (0, 2, 4, 6, 8 and 10 μM) in the wavelength difference of $\Delta\lambda = 15$ nm. Arrow shows the emission intensity changes upon the increasing concentration of compounds.

cancer cell lines. The IC_{50} values indicated that the cytotoxic activity of **3** is greater than that of **2**. The comparative study of the pharmacological properties of two new Cu(II) complexes do indicate a superior activity for **3** which might be due to the cationic nature of the octahedral complex (**3**) over the neutral square pyramidal geometry of (**2**). The findings are significant for exploring further the DNA and protein interaction, antioxidative and cytotoxic activities of the transition metal complexes containing different 2-oxo-1,2-dihydroquinoline-3-carbaldehyde Schiff-bases.

4. Experimental

4.1. Materials and instrumentation

All starting precursors were of analytical grade and double-distilled water was used throughout the experiments. 2-oxo-1,2-dihydroquinoline-3-carbaldehyde was prepared according to the literature procedure [48]. The reagents and solvents were purchased commercially and used without further purification unless otherwise noted. CT-DNA, BSA and EB were obtained from Sigma–Aldrich and used as received. Elemental analyses (C, H, N) were performed on Vario EL III Elemental analyzer instrument. IR spectra ($4000\text{--}400\text{ cm}^{-1}$) for were recorded on a Nicolet Avatar Model FT-IR spectrophotometer. ^1H NMR spectrum of the ligand was recorded on Bruker AMX 500 at 500 MHz. Melting points were determined with a Lab India instrument. Electronic absorption spectra were recorded using Jasco V-630 spectrophotometer. Emission spectra were measured with Jasco FP 6600 spectrofluorometer. Solid state magnetic susceptibility measurements were carried out at room temperature on a Faraday balance calibrated using mercury(II) tetrathiocyanatocobaltate(II) as a calibrant.

4.2. Preparation of compounds

4.2.1. Synthesis of 2-oxo-1,2-dihydroquinoline-3-carbaldehyde (benzoyl) hydrazone

It was prepared by the method described with some modifications [17]. Benzohydrazide (1.36 g, 0.01 mol) dissolved in warm methanol (50 mL) was added to a methanol solution (50 mL) containing 2-oxo-1,2-dihydroquinoline-3-carbaldehyde (1.73 g, 0.01 mol). The mixture was refluxed for an hour during which a yellow precipitate was formed. The reaction mixture was then cooled to room temperature and the solid formed was filtered. It was then washed with methanol and dried under vacuum.

Yield, 92%. M.p. $314\text{--}316\text{ }^\circ\text{C}$. Elemental Analysis: Found (calculated) (%) for $\text{C}_{17}\text{H}_{13}\text{N}_3\text{O}_2$: C, 70.01 (70.09); H, 4.59 (4.50); N, 14.41 (14.42). UV–visible (solvent: MeOH): λ_{max} (nm): 326, 363 ($\pi \rightarrow \pi^*$ & $n \rightarrow \pi^*$). IR: ν_{max} (cm^{-1}): $\nu_{\text{C=O}}$: 1653, $\nu_{\text{C=N}}$: 1546. ^1H NMR (DMSO- d_6 500 MHz, s, singlet; d, doublet; t, triplet; m, multiplet): 12.03 (s, 1H, N(3)H); 12.01 (s, 1H, N(2)H); 8.74 (s, 1H, C(1)H); 8.50 (s, 1H, C(6)H); 7.95–7.97 (d, 2H, C(13,17)H); 7.87–7.90 (d, 1H, C(10)); 7.60–7.62 (t, 1H, C(9)H); 7.53–7.59 (m, 3H, C(14,15,16)H); 7.35–7.37 (d, 1H, C(7)H); 7.22–7.26 (t, 1H, C(8)H).

4.2.2. Synthesis of the complexes

Complexes **2** and **3** were synthesized by refluxing equimolar amount of ethanolic solutions of appropriate metal salts $\text{CuCl}_2 \cdot 2\text{H}_2\text{O}$ (85 mg, 0.5 mmol) or $\text{Cu}(\text{NO}_3)_2 \cdot 3\text{H}_2\text{O}$ (121 mg, 0.5 mmol) with the methanolic solution of ligand **1** (146 mg, 0.5 mmol) for 30 min (Scheme 1). Green coloured crystals suitable for X-ray studies were obtained on slow evaporation of the reaction mixture in both the cases. They were filtered off, washed with cold methanol, and dried under vacuum.

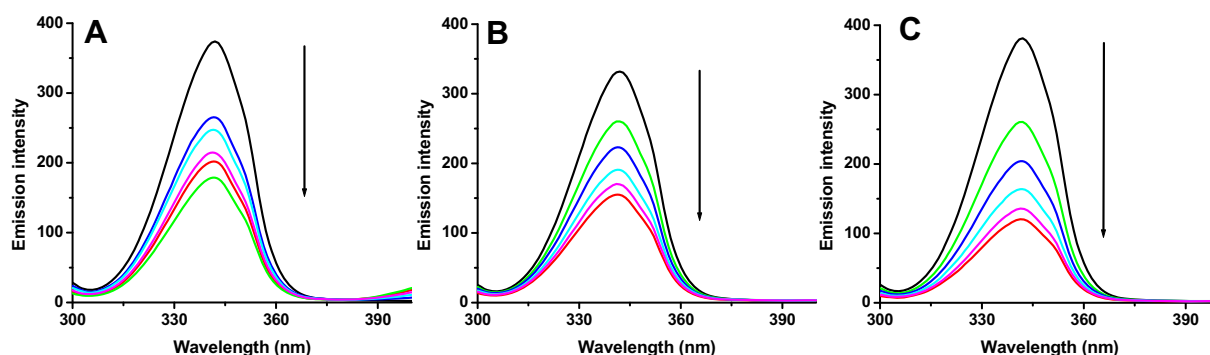


Fig. 10. Synchronous spectra of BSA (1 μM) in the presence of increasing amounts of compounds **1** (A), **2** (B) and **3** (C) (0, 2, 4, 6, 8 and 10 μM) in the wavelength difference of $\Delta\lambda = 60$ nm. Arrows show the emission intensity decreases upon the increasing concentration of compounds.

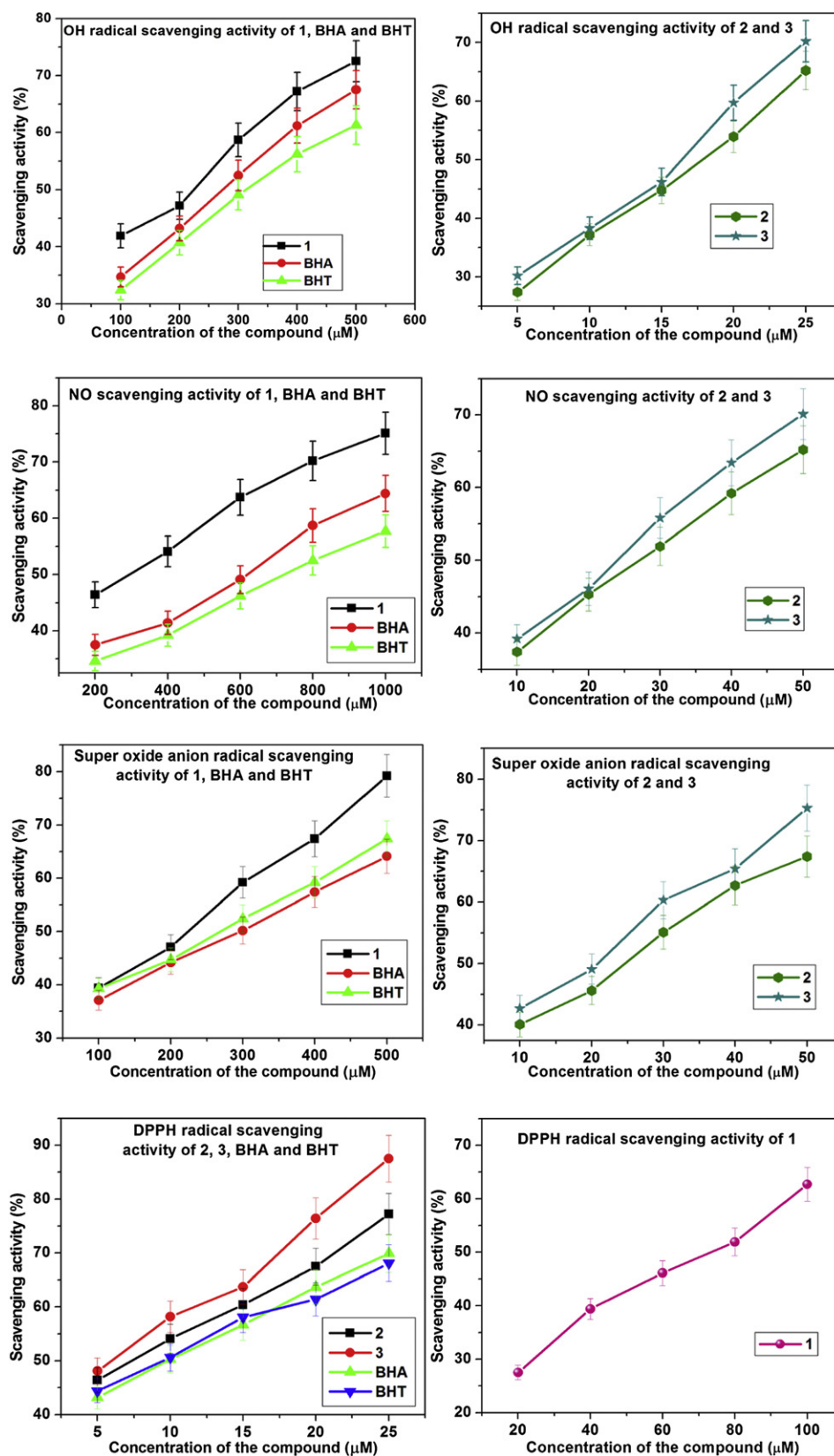


Fig. 11. The OH radical, NO, superoxide anion radical, and 2,2'-diphenyl-1-picrylhydrazyl (DPPH) radical, scavenging activity at various concentrations of the compounds (1, 2 and 3) and the standards, butylatedhydroxyanisole (BHA) and butylatedhydroxytoluene (BHT).

Table 4
The radical scavenging activity of the compounds.

Compounds	IC ₅₀ values (μM)			
	OH•	NO	DPPH•	O ₂ •
1	219 ± 7	293 ± 7	77.5 ± 2.1	225 ± 4
2	17.7 ± 1.2	27.5 ± 2.7	7.3 ± 1.1	25.1 ± 2.3
3	16.5 ± 3.7	24.4 ± 3.2	6.23 ± 0.91	20.9 ± 1.9
BHA	274 ± 9	623 ± 10	9.84 ± 0.83	296 ± 7
BHT	312 ± 8	725 ± 9	9.92 ± 0.64	274 ± 6

Complex **2**: Yield, 82%. M.p. 327–330 °C. Elemental Analysis: Found (calculated) (%) for C₁₇H₁₇Cl₂CuN₃O₄: C, 44.37 (44.22); H, 3.71 (3.71); N, 9.11 (9.10). UV–visible (solvent: MeOH): λ_{max} (nm): 261 (ILCT), 365 (ILCT), 401 (LMCT), 423 (MLCT). IR: ν_{max} (cm⁻¹): ν_{C=O}: 1643, ν_{C=N}: 1554. μ_{eff} (300K): 1.77 μ_B.

Complex **3**: Yield, 85%. M.p. 334–336 °C. Elemental Analysis: Found (calculated) (%) for C₁₉H₂₃CuN₅O₁₁: C, 40.62 (40.68); H, 4.21 (4.13); N, 12.47 (12.48). UV–visible (solvent: MeOH): λ_{max} (nm): 260 (ILCT), 366 (ILCT), 400 (LMCT), 421 (MLCT). IR: ν_{max} (cm⁻¹): ν_{C=O}: 1629, ν_{C=N}: 1548. μ_{eff} (300K): 1.74 μ_B.

4.3. Crystallography

Single-crystal X-ray diffraction data of **2** and **3** were collected on BRUKER SMART 1000 X-ray (three-circle) diffractometer. Integrated intensity information for each reflection was obtained by reduction of the data frames with the program APEX2 [49]. In **2**, the hydrogen atoms bound to carbon and nitrogen were placed in idealized positions, hydrogen bound to oxygen (water) were either located from Fourier difference map (for O30) or modeled with idealized distance (for O40) and were set riding. O40 refined with occupancy near 0.5 and was fixed at that value. In **3**, ethanol molecule shows longer than usual bond lengths. It could be either ethanol, or disordered methanol, or a disorder of methanol and ethanol. The hydrogen atom attached to the ethanol molecule is only modeled for formula considerations. Thermal parameters of the N(40)O₃ group showed unusually elongated motions. Hydrogen atoms attached to N and O were located from the Fourier difference maps and was set riding on the respective parent atom. All non-hydrogen atoms were refined with anisotropic thermal parameters. The structures were refined (weighted least-squares refinement on F²) to convergence [50].

4.4. DNA interaction experiments

All the experiments involving the binding of compounds **1**, **2** and **3**, with CT-DNA were carried out in a doubly distilled water buffer with tris(hydroxymethyl)-aminomethane (Tris, 5 mM) and sodium chloride (50 mM) and adjusted to pH 7.2 with hydrochloric acid. A solution of CT-DNA in the buffer gave a ratio of UV absorbance of about 1.9 at 260 and 280 nm, indicating that the DNA was sufficiently free of protein. The DNA concentration per nucleotide was determined by absorption spectroscopy using the molar extinction coefficient value of 6600 dm³ mol⁻¹ cm⁻¹ at 260 nm. The compounds were dissolved in a mixed solvent of 5% DMSO and 95%

Table 5
The cytotoxic activity of the compounds.

Compounds	IC ₅₀ Values (μM)			
	HeLa	HEp-2	Hep G2	NIH 3T3
2	37.7 ± 1.2	47.5 ± 2.7	17.1 ± 1.2	245 ± 6
3	26.5 ± 1.7	34.3 ± 2.2	16.3 ± 0.7	271 ± 6
Cisplatin	12.1 ± 0.6	14.7 ± 0.9	9.91 ± 0.43	274 ± 6

Tris–HCl buffer. Absorption titration experiments were performed with fixed concentrations of the compounds (25 μM) with varying concentration of DNA (2.5–25 μM). While measuring the absorption spectra, an equal amount of DNA was added to both the test solution and the reference solution to eliminate the absorbance of DNA itself. The same experimental procedure was followed for emission studies also. The ligand (**1**) and its complexes **2** and **3** were excited at 365 and 400 nm respectively and their corresponding emission spectra were monitored. EB-DNA experiments were conducted by adding the solution of the compounds to the Tris–HCl buffer of EB-DNA. The change of fluorescence intensity was recorded. The excitation and the emission wavelength were 515 nm and 602 nm, respectively.

4.5. Protein binding studies

Binding of the test compounds **1**, **2** and **3** with bovine serum albumin (BSA) was studied using fluorescence spectra recorded with an excitation at 280 nm and corresponding emission at 344 nm assignable to that of free bovine serum albumin (BSA). The excitation and emission slit widths and scan rates were maintained constant for all the experiments. Samples were carefully degassed using pure nitrogen gas for 15 min. Quartz cells (4 × 1 × 1 cm) with high vacuum Teflon stopcocks were used for degassing. Stock solution of BSA was prepared in 50 mM phosphate buffer (pH = 7.2) and stored in the dark at 4 °C for further use. Concentrated stock solution of compounds were prepared by dissolving the compounds in DMSO:phosphate buffer (1:50) and diluted suitably with phosphate buffer to required concentrations for all the experiments. Titrations were manually done by using micropipette for the addition of compounds. For synchronous fluorescence spectra also, the same concentration of BSA and compounds were used and the spectra were measured at two different Δλ (difference between the excitation and emission wavelengths of BSA) values such as 15 and 60 nm.

4.6. Antioxidant assays

The DPPH radical scavenging activity of the compounds was measured according to the method of Blios [51]. The DPPH radical is a stable free radical having λ_{max} at 517 nm. A variable concentration of the test compounds was added to a solution of DPPH in methanol (125 μM, 2 mL) and the final volume was made up to 4 mL with double-distilled water. The solution was incubated at 37 °C for 30 min in dark. The decrease in absorbance of DPPH was measured at 517 nm. The same experiment carried out without the test compounds served as control.

The hydroxyl radical scavenging activities of the compounds have been investigated using the Nash method [52]. *In vitro* hydroxyl radicals were generated by Fe³⁺/ascorbic acid system. The detection of hydroxyl radicals was carried out by measuring the amount of formaldehyde formed from the oxidation reaction with DMSO. The formaldehyde produced was detected spectrophotometrically at 412 nm. A mixture of 1.0 mL of iron-EDTA solution (0.13% ferrous ammonium sulphate and 0.26% EDTA), 0.5 mL of EDTA solution (0.018%), and 1.0 mL of DMSO (0.85% DMSO (v/v) in 0.1 M phosphate buffer, pH 7.4) were sequentially added in the test tubes containing the test compounds with variable concentrations. The reaction was initiated by adding 0.5 mL of ascorbic acid (0.22%) and incubated at 80–90 °C for 15 min in a water bath. After incubation, the reaction was terminated by the addition of 1.0 mL of ice-cold TCA (17.5% w/v). Subsequently, 3.0 mL of Nash reagent was added to each tube and left at room temperature for 15 min. The intensity of the colour formed was measured spectrophotometrically at 412 nm against reagent blank.

Assay of nitric oxide scavenging activity is based on the method [53], where sodium nitroprusside in aqueous solution at physiological pH spontaneously generates nitric oxide, which interacts with oxygen to produce nitrite ions that can be estimated using Griess reagent. Scavengers of nitric oxide compete with oxygen leading to reduced production of nitrite ions. For the experiment, sodium nitroprusside (10 mM) in phosphate buffered saline was mixed with a variable concentration of the compounds and incubated at room temperature for 150 min. After the incubation period, 0.5 mL of Griess reagent containing 1% sulfanilamide, 2% H₃PO₄ and 0.1% N-(1-naphthyl) ethylenediaminedihydrochloride were added. The absorbance of the chromophore formed was measured at 546 nm. The same experiment carried out without the test compounds served as control.

The superoxide anion radical scavenging assay was based on the capacity of the compounds to inhibit formazan formation by scavenging the superoxide radicals generated in riboflavin-light-NBT system [54]. Each 3 mL reaction mixture contained 50 mM sodium phosphate buffer (pH 7.6), 20 µg riboflavin, 12 mM EDTA, 0.1 mg NBT and 1 mL complex solution (20–100 µg/mL). Reaction was started by illuminating the reaction mixture with various concentrations of the test compounds for 90 s. Immediately after illumination, the absorbance was measured at 590 nm. The entire reaction assembly was enclosed in a box lined with aluminum foil. Identical tubes with reaction mixture kept in dark served as blanks.

For the above four assays, blank samples containing same volume of DMSO which is used to dissolve the compounds are taken as controls; all the tests were run in triplicate and various concentrations of the compounds were used to fix a concentration range at which compounds showed in and around 50% of activity. In addition, the percentage of activity was calculated using the formula, % of activity = $[(A_0 - A_c)/A_0] \times 100$ (A_0 and A_c are the absorbance in the absence and presence of the tested complex respectively). The 50% of activity (IC_{50}) was calculated using the percentage of activity results.

4.7. Cytotoxicity assay

Cytotoxicity studies of the compounds and cisplatin were carried out on human cervical cancer cell line (HeLa), human laryngeal epithelial carcinoma cells (HEp-2), and human liver carcinoma cells (Hep G2) along with one normal mouse embryonic fibroblasts cell line (NIH 3T3) which were obtained from National Centre for Cell Science, Pune, India. Cell viability was carried out using the MTT (3-(4,5-Dimethylthiazol-2-yl)-2,5-diphenyltetrazolium bromide) assay method [55]. The HeLa, HEp-2 and Hep G2 cells were grown in Eagles minimum essential medium containing 10% fetal bovine serum (FBS). NIH 3T3 fibroblasts were grown in Dulbeccos Modified Eagles Medium (DMEM) containing with 10% FBS. For screening experiment, the cells were seeded into 96 -well plates in 100 µl of respective medium containing 10% FBS, at plating density of 10,000 cells/well and incubated at 37 °C, 5% CO₂, 95% air and 100% relative humidity for 24 h prior to addition of compounds. The compounds were dissolved in DMSO and diluted in respective medium containing 1% FBS. After 24 h, the medium was replaced with respective medium with 1% FBS containing the compounds at various concentration (5–500 µM) and incubated at 37 °C, 5% CO₂, 95% air and 100% relative humidity for 48 h. Triplicate was maintained and the medium containing without the test compounds were served as control. After 48 h, 10 µl of MTT (5 mg/mL) in phosphate buffered saline (PBS) was added to each well and incubated at 37 °C for 4 h. The medium with MTT was then flicked off and the formed formazan crystals were dissolved in 100 µl of DMSO and then measured the absorbance at 570 nm using micro plate reader. The amount of DMSO used to dissolve the tested

compounds has been maintained as less than 5% of the total concentration for all the experiments. The % of cell inhibition was determined using the following formula and graph was plotted between % of cell inhibition and concentration and from this IC_{50} value was calculated. % inhibition = $[\text{mean OD of untreated cells (control)}/\text{mean OD of treated cells (control)}] \times 100$.

Acknowledgments

Financial assistance received from the Council of Scientific and Industrial Research, New Delhi, India [Grant No. 01(2216)/08/EMR-II & 21(0745)/09/EMR-II], is gratefully acknowledged.

Appendix. Supplementary material

Supplementary data related to this article can be found online at doi:10.1016/j.jmech.2011.10.024.

References

- [1] R.A. Sanchez-Delgado, M. Navarro, H. Perez, J.A. Urbina, *J. Med. Chem.* 39 (1996) 1095–1099.
- [2] J.A. Drewry, P.T. Gunning, *Coord. Chem. Rev.* 255 (2011) 459–472.
- [3] V. Milacic, Q.P. Dou, *Coord. Chem. Rev.* 253 (2009) 1649–1660.
- [4] R. Malhotra, J.P. Singh, M. Dudeja, K.S. Dhindsa, *J. Inorg. Biochem.* 46 (1992) 119–127.
- [5] D.R. Richardson, *Antimicrob. Agents Chemother.* 41 (1997) 2061–2063.
- [6] F. Lebon, M. Ledecq, Z. Benatallah, S. Sicsic, R. Lapouyade, O. Kahan, A. Garcon, M. Reboud-Ravaux, F. Durant, *J. Chem. Soc. Perkin Trans. 2* (1999) 795–800.
- [7] N. Bharti, M.R. Maurya, F. Naqvi, A. Bhattacharya, S. Bhattacharya, A. Azam, *Eur. J. Med. Chem.* 35 (2000) 481–486.
- [8] P. Krishnamoorthy, P. Sathyadevi, A.H. Cowley, R.R. Butorac, N. Dharmaraj, *Eur. J. Med. Chem.* 46 (2011) 3376–3387.
- [9] D.S. Raja, N.S.P. Bhuvanesh, K. Natarajan, *J. Biol. Inorg. Chem.*, doi:10.1007/s00775-011-0844-1.
- [10] Y.-C. Liu, Z.-Y. Yang, *Eur. J. Med. Chem.* 44 (2009) 5080–5089.
- [11] Y.-C. Liu, Z.-Y. Yang, *J. Inorg. Biochem.* 103 (2009) 1014–1022.
- [12] S. Banerjee, S. Mondal, W. Chakraborty, S. Sen, R. Gachhui, R.J. Butcher, A.M.Z. Slawin, C. Mandal, S. Mitra, *Polyhedron* 28 (2009) 2785–2793.
- [13] C.D. Fan, H. Su, J. Zhao, B.X. Zhao, S.L. Zhang, J.Y. Miao, *Eur. J. Med. Chem.* 45 (2010) 1438–1446.
- [14] Y. Li, Z.-Y. Yang, *Inorg. Chim. Acta* 362 (2009) 4823–4831.
- [15] Z.-C. Liu, B.-D. Wang, Z.-Y. Yang, Y. Li, D.D. Qin, T.-R. Li, *Eur. J. Med. Chem.* 44 (2009) 4477–4484.
- [16] D.S. Raja, G. Paramaguru, N.S.P. Bhuvanesh, J.H. Reibenspies, R. Renganathan, K. Natarajan, *Dalton Trans.* 40 (2011) 4548–4559.
- [17] Z.-C. Liu, B.-D. Wang, B. Li, Q. Wang, Z.-Y. Yang, T.-R. Li, Y. Li, *Eur. J. Med. Chem.* 45 (2010) 5353–5361.
- [18] A.W. Addison, T.N. Rao, J. Reedijk, J. van Rijn, G.C. Veschoor, *J. Chem. Soc. Dalton Trans.* (1984) 1349–1356.
- [19] E.C. Miller, J.A. Miller, *Cancer* 47 (1981) 1055–1064.
- [20] A.E. Friedman, C.V. Kumar, N.J. Turro, J.K. Barton, *Nucleic Acids Res.* 19 (1991) 2595–2602.
- [21] A.M. Pyle, T. Morri, J.K. Barton, *J. Am. Chem. Soc.* 112 (1990) 9432–9434.
- [22] J.K. Barton, J.M. Goldberg, C.V. Kumar, N.J. Turro, *J. Am. Chem. Soc.* 108 (1986) 2081–2088.
- [23] P.H. Proctor, E.S. Reynolds, *Physiol. Chem. Phys. Med. NMR.* 16 (1984) 175–195.
- [24] K.E. Erkkila, D.T. Odom, J.K. Barton, *Chem. Rev.* 99 (1999) 2777–2795.
- [25] B.N. Trawick, A.T. Danihe, J.K. Bashkin, *Chem. Rev.* 98 (1998) 939–960.
- [26] J.K. Barton, A.T. Danishefsky, J.M. Goldberg, *J. Am. Chem. Soc.* 106 (1984) 2172–2176.
- [27] F.Q. Liu, Q.X. Wang, K. Jiao, F.F. Jian, G.Y. Liu, R.X. Li, *Inorg. Chim. Acta* 359 (2006) 1524–1530.
- [28] D. Lawrence, V.G. Vaidyanathan, B.U. Nair, *J. Inorg. Biochem.* 100 (2006) 1244–1251.
- [29] D.S. Raja, N.S.P. Bhuvanesh, K. Natarajan, *Eur. J. Med. Chem.* 46 (2011) 4584–4594.
- [30] M. Eriksson, M. Leijon, C. Hiort, B. Norden, A. Graeslund, *Biochemistry* 33 (1994) 5031–5040.
- [31] A. Wolf, G.H. Shimer, T. Meehan, *Biochemistry* 26 (1987) 6392–6396.
- [32] G. Zhao, H. Lin, S. Zhu, H. Sun, Y. Chen, *J. Inorg. Biochem.* 70 (1998) 219–226.
- [33] M. Howe-Grant, K.C. Wu, W.R. Bauer, S.J. Lippard, *Biochemistry* 15 (1976) 4339–4446.
- [34] F.J. Meyer-Almes, D. Porschke, *Biochemistry* 32 (1993) 4246–4253.
- [35] G.M. Howe, K.C. Wu, W.R. Bauer, *Biochemistry* 19 (1976) 339–347.
- [36] Y.B. Zeng, N. Yang, W.S. Liu, N. Tang, *J. Inorg. Biochem.* 97 (2003) 258–264.
- [37] B.D. Wang, Z.-Y. Yang, Q. Wang, T.K. Cai, P. Crewdson, *Bioorg. Med. Chem.* 14 (2006) 1880–1888.

- [38] B.P. Kamat, J. Seetharamappa, *J. Pharm. Biomed. Anal.* 35 (2008) 655–664.
- [39] X.Z. Feng, Z. Yang, L.J. Wang, C. Bai, *Talanta* 47 (1998) 1223–1229.
- [40] G.Z. Chen, X.Z. Huang, Z.Z. Zheng, J.G. Xu, Z.B. Wang, *Methods of Fluorescence Analysis*, second ed. Science Press, Beijing, 1990.
- [41] J.N. Miller, *Proc. Anal. Div. Chem. Soc.* 16 (1979) 203–208.
- [42] J.H. Tang, F. Luan, X.G. Chen, *Bioorg. Med. Chem.* 149 (2006) 3210–3217.
- [43] M. Sankaran, C. Kumarasamy, U. Chokkalingam, P.S. Mohan, *Bioorg. Med. Chem. Lett.* 20 (2010) 7147–7151.
- [44] M.G. Malakyan, S.A. Badzhinyan, L.A. Vardevanyan, D.S. Grigoryan, D.E. Egiazaryan, A.A. Avetisyan, I.L. Aleksanyan, L.P. Ambartsumyan, K.S. Sargsyan, *Pharm. Chem. J.* 43 (2009) 8–11.
- [45] A. Ahmad, S.F. Asad, S. Singh, S.M. Hadi, *Cancer Lett.* 154 (2000) 29–37.
- [46] A.S. Azmi, S.H. Bhat, S.M. Hadi, *FEBS Lett.* 579 (2005) 3131–3135.
- [47] S.H. Bhat, A.S. Azmi, S.M. Hadi, *Toxicol. Appl. Pharmacol.* 218 (2007) 249–255.
- [48] M.K. Singh, A. Chandra, B. Singh, R.M. Singh, *Tetrahedron Lett.* 48 (2007) 5987–5990.
- [49] APEX2 "Program for Data Collection on Area Detectors" BRUKER AXS Inc. 5465 East Cheryl Parkway, Madison, WI 53711–5373 USA.
- [50] G.M. Sheldrick, *SADABS (Version 2008/1): Program for Absorption Correction for Data from Area Detector Frames*. University of Gottingen, 2008.
- [51] M.S. Blois, *Nature* 29 (1958) 1199–1200.
- [52] T. Nash, *Biochem. J.* 55 (1953) 416–421.
- [53] L.C. Green, D.A. Wagner, J. Glogowski, P.L. Skipper, J.S. Wishnok, S.R. Tannenbaum, *Anal. Biochem.* 126 (1982) 131–138.
- [54] C. Beauchamp, I. Fridovich, *Anal. Biochem.* 44 (1971) 276–287.
- [55] M. Blagosklonny, W.S. El-diery, *Int. J. Cancer* 67 (1996) 386–392.